

# Lawrence Berkeley National Laboratory

## Lawrence Berkeley National Laboratory

### **Title**

APPARATUS TO DETECT STABLE FRACTIONAL CHARGES ON MATTER

### **Permalink**

<https://escholarship.org/uc/item/4k3463rb>

### **Author**

Vanderspek, R.

### **Publication Date**

1980-04-01

Peer reviewed

# Apparatus to Detect Stable Fractional Charges on Matter

*Roland Vanderspek*  
Lawrence Berkeley Laboratory  
University of California  
Berkeley, California 94720

## 1. Introduction

In the early years of this century, Millikan demonstrated that the electric charges on tiny droplets of oil were quantized. With this discovery he confirmed that matter was made up of particles charged with integral-multiples of a basic charge unit  $e=4.80 \times 10^{-10}$  *esu*. In the mid-60's Gell-Mann and Zweig proposed a theory of hadron structure based on three types of quarks, objects which are most easily interpreted as particles with charges of  $\pm \frac{1}{3}e$  or  $\pm \frac{2}{3}e$ . Later experiments bore out the theory by showing that hadrons appear to be composed of point-like fractionally-charged particles. One question raised by these results is that of the existence of an isolated quark in nature. There have been many searches for fractionally-charged particles produced in high-energy accelerator reactions and in even higher-energy cosmic-ray events, but they have yielded no positive results.<sup>2</sup> If quarks exist at all in isolation, there is reason to believe that they will be found in some concentration in the Earth's crust. The quarks would most likely be the result of some super-high-energy cosmic-ray event or the relics of some early stage of the formation of the universe. Many searches for isolated quarks on stable matter have been undertaken, again with no positive results.<sup>2</sup> The total amount of matter examined directly in the searches to date is a few milligrams. An apparatus is described here which will analyze matter for stable fractional charges in quantities ranging around one gram. A rate of mass-analysis of  $10^{-4}$  g/sec and an ultimate sensitivity of  $10^{-24}$  per nucleon are expected.

## 2. Theory of Apparatus

The apparatus analyzes the charges of a series of droplets by measuring their deflection in falling through a horizontal static electric field. The force on a droplet is

$$\vec{F}(q, \vec{x}, \vec{v}, neighbors) = m\vec{g} + q\vec{E}(\vec{x}) - m\vec{v}\vec{v}(\vec{x}) + \vec{p} \cdot \vec{\nabla}E + \vec{\mu} \cdot \vec{\nabla}B + \vec{F}_{neighbors}$$

where  $q$  = charge on droplet

$\vec{v}$  = velocity of droplet

$m$  = mass of droplet

$\vec{g}$  = gravitational acceleration

$\vec{\nabla}E$  = electric field gradient

$\vec{\nabla}B$  = magnetic field gradient

$\nu$  = drag coefficient

$\vec{p}$  = electric dipole moment of droplet

$\vec{\mu}$  = magnetic dipole moment of droplet.

The term  $\vec{F}_{neighbors}$  is the total force due to the electrical and aerodynamic interactions with nearby droplets in the apparatus. These electrical interactions are between the respective charges and dipole moments of neighboring droplets. The dominant term in  $\vec{F}_{neighbors}$  is that of the dipole-dipole interaction between adjacent droplets. The magnitude of these forces decreases with distance, so minimization of their effects requires the maintenance of a minimum separation between droplets. This allows the simplification of the dependence of the force on a droplet to  $\vec{F}(q, \vec{v}, \vec{x})$ . The net deflection of a droplet by this force is

$$\delta x = \frac{qV_0L^2}{mv^2b},$$

where  $V_0$  = potential on the deflecting electrodes

$L$  = length of deflecting electrodes

$b$  = mean separation between deflecting electrodes

$v$  = characteristic velocity of droplet.

In the ideal case, where all parameters besides droplet charge are repeatable, the deflection of all droplets of a given charge due to this force is the same for each droplet, and the precision of resolution of the charge is limited only by the resolution in the measurement of the deflection. In actuality, the deflection of a given charge varies with the parameters. High charge resolution requires high consistency in these parameters; *i.e.* the variations  $\delta m/m$  and  $\delta v/v$  among all droplets must be kept small. The existence of a divergent spray in the stream of droplets introduces an essentially random component of velocity perpendicular to the flow to the droplets. All perpendicular velocities must be kept to an absolute minimum, since a small velocity, multiplied by a time-of-flight of the order of a second, can result in a noticeable variance in the deflection of a droplet. It is also important that none of the forces or parameters change with

time. Such time-variations would change the deflection of droplets of a given charge from one droplet to the next and thereby lower the resolution of analysis.

The series of droplets is formed from a stream of liquid emitted by the apparatus. The production of droplet jets from streams of liquid depends on the tendency of a liquid to minimize its surface energy by minimizing its surface area. The lowest surface energy configuration of a given volume of liquid is a single sphere. A cylindrical stream of radius  $a$  can therefore lower its surface energy by breaking up into a series of identical spheres of separation  $d$  for certain values of  $d$ . The ratio of surface area of the stream to that of the spheres is proportional to  $(d/a)^{1/3}$ . Exact analysis reveals that the stream is energetically favored to break up into droplets with  $d > 4.5a$ . The existence of such lower surface energy configurations makes the stream inherently unstable. Thus, the proper perturbations to the surface of the stream will grow to achieve these configurations.

Because of the instability of the stream, a capillary wave applied to its surface will grow in amplitude until droplets are formed (see Figure 1). For the purposes of calculation, we assume the capillary wave to be a small sinusoidal perturbation whose amplitude grows as  $e^{vt}$ . In the growth process, the surface potential energy of the stream decreases as the surface area decreases, while, at the same time, certain parts of the stream experience an increase in kinetic energy in contracting into droplets. Conservation of energy leads to the equation

$$v^2 = \text{constant} \times \left( \frac{\pi k^2}{V/L} - k^4 \right)$$

where  $k$  is the wave number of the perturbation and  $V/L$  is the volume per unit length of the stream. This function has a sharp maximum,  $v_{\text{max}}$ , at a certain wavelength perturbation,  $k_{\text{optimal}}$  (see Figure 2). This wavelength corresponds to a capillary-wave frequency of  $\omega_{\text{optimal}} = vk_{\text{optimal}}$ , where  $v$  is the velocity of the stream. The growth rates of higher harmonics of this frequency,  $\omega_{\text{harmonic}} = N\omega_{\text{optimal}}$ , for integer  $N$ , are negligible compared to  $v_{\text{max}}$ . Thus, when  $\omega_{\text{optimal}}$  is found in combination with higher harmonics in a complex perturbation it is the dominant frequency, and the effects of the higher perturbation frequencies are negligible. Sub-harmonic perturbations, on the other hand, could introduce cyclic variations in the droplet parameters. The droplet radius  $r$ , the droplet separation  $d$  and  $k_{\text{optimal}}$  are all functions of the stream radius  $a$ . In the simple approximation presented above,  $k_{\text{optimal}} = 0.707/a$ . A perturbation of this wave number produces droplets of radius  $r = 1.88a$  and separation  $d = 4.72r$ . In actual practice,  $k_{\text{optimal}} \approx 0.70/a$ , producing droplets of  $r \approx 1.89a$  and  $d \approx 4.77r$ .<sup>3</sup>

Non-linear effects associated with certain combinations in wavelength and amplitude capillary-wave perturbations are conducive to the formation of smaller, satellite droplets between adjacent primary droplets (see Figure 1d). It is beyond the scope of this paper to go

into the details of this phenomenon, as the theory of the formation of satellites has not yet been developed. Figure 3 is a plot of data collected by researchers at *IBM* and indicates the frequency-amplitude window in which satellites are created.<sup>4</sup> At amplitudes above the window, the satellites will forward-merge within a few wavelengths; at those below the window, the satellites backward-merge in the same range. The diameter of a satellite droplet is generally about one tenth the diameter of a primary droplet.

A charge can be induced on a droplet by applying a potential to an electrode surrounding the stream at the point of separation. The electrically conductive liquid in the stream is held near zero potential; thus, the potential on the electrode draws charges into the tip of the stream. The magnitude of the mean charge induced on the droplet depends on the capacitance between the droplet and the electrode and the capacitances between the droplet and previously released droplets. Thermal fluctuations produce a distribution of charges around this mean charge. The *rms* deviation of the distribution of the charges on a capacitor  $C$  in equilibrium with a temperature bath  $T$  is equal to  $\sqrt{2CkT}$ . For an isolated spherical droplet, the capacitance is just the droplet radius.

### 3. Description of Method

The apparatus, which is diagrammed in Figure 4, can operate in two modes. Both modes produce droplets at rates corresponding to maximum growth of capillary-wave perturbations. The first mode produces a series of small, identical droplets of which only a small percentage is retained for analysis. These droplets are given a mean charge of zero; the thermally-induced deviations about this mean are analyzed. The remaining droplets are charged highly and deflected from between the deflecting electrodes in order to increase the separation between analyzed droplets. A small slot in each of the deflecting electrodes facilitates the disposal of these and other highly-charged droplets.

The second mode operates in the satellite-creation window (see Figure 3), and produces satellites between primary droplets comparable in size to the primary droplets of mode 1. A larger orifice produces larger, more-widely separated primary droplets than in mode 1. All droplets are given zero mean charge, and the satellite droplets are charge-analyzed as above. The primary droplets are removed from analysis by striking and wetting a small silver-plated sphere before passing between the deflecting electrodes. This sphere makes grazing contact with the primary droplets and no contact with the satellites. The primary droplets adhere to the wetted surface and are carried along the sphere, being released from the surface after experiencing deflections of about 30 degrees. The liquid of the droplet collects in a doughnut-shaped well surrounding the stream of smaller droplets. The well also serves to collect mercury dripping from the silvered sphere. The liquid in this well flows through a drain into a second well, from

which it flows out of the apparatus through a section of stainless steel pipe. The primary droplets can also be allowed to travel with the satellites, falling essentially undeflected through the apparatus. In both modes analyzed droplets maintain at least the separation calculated to reduce adequately the effects of electrical and aerodynamic interactions. This separation is approximately  $650 \mu m$  for  $10 \mu m$  drops.<sup>1</sup>

The capillary-wave perturbation to the surface of the stream is provided by two piezoelectric crystals. An oscillating potential across the crystals causes them to vibrate parallel to their axis as in Figure 5. The longitudinal vibrations of the crystals and the throat of the droplet generator coupled with the induced vibrations in the stream and orifice introduce harmonic perturbations of higher frequencies to the stream. These harmonics and the variations of the driving signal from a pure sinusoid have little effect on the formation of droplets. The dynamics of capillary-wave growth, as discussed above, emphasizes only one of the set of harmonics making up a complex wave-form, and thus renders higher harmonics harmless.

#### 4. Apparatus

The droplet generator is made of electron-beam welded *AISI* 412 stainless steel. It is diagrammed in Figures 4 and 6. In mode 1, the droplet generator produces on the order of  $10^5$  droplets of mercury per second, with a  $10 \mu m$ -diameter orifice producing  $20 \mu m$ -diameter droplets. The orifice from which the stream is emitted is a small hole drilled into a thin stainless steel sheet. In mode 2, the droplet generator produces  $\approx 10^4$   $200 \mu m$  droplets/sec from a  $100 \mu m$  orifice. In both cases the initial velocity of the droplets is near  $500 \text{ cm/sec}$ . The droplet generator produces droplets measured consistent to  $\delta v/v < 10^{-3}$ ,  $\delta m/m < 10^{-3}$  and  $\delta v_{perp}/v < 10^{-6}$ , where  $v_{perp}$  is the component of droplet velocity perpendicular to the flow of droplets. The stream of droplets may be observed before deflection with a microscope situated above the deflecting electrodes.

The charging electrode is a cylinder of high-transparency etched nickel mesh concentric to the stream of liquid at the point of separation of the droplets. Application of a  $3 \text{ mV}$  potential to the charging electrode will induce a mean charge of  $10e$  on a droplet. The charge induced on a droplet is highly sensitive to changes in the potential applied to the charging electrode; hence, the applied potential must be very accurate in order to be able consistently to induce the same mean charge on each of a series of droplets. In mode 1, approximately 29 of every 30 droplets are charged to about  $300e$  by the application of a  $0.1 \text{ V}$  potential to the charging electrode. These droplets are deflected from between the deflecting electrodes within a distance of  $3 \text{ cm}$ . This stream of droplets is inherently unstable because of the mutual repulsion of the charges on the droplets. The application of higher charges to these droplets would increase this instability and thereby increase the magnitude of their random effects on the trajectories of the analyzed

droplets. The induction of zero mean charge on the remaining droplet requires the application of a potential to the charging electrode to cancel the contact potentials on the stream. The magnitude of this potential is roughly 0.5 V. The *rms* deviation from zero charge due to thermal effects is calculated to be approximately  $\pm 18e$  on  $10\mu m$  droplets. This calculation has been independently verified by Roger Bland of San Francisco State University, who measured an *rms* deviation of  $\pm 12e$  on  $5\mu m$  droplets.<sup>5</sup>

The initial signal to the charging electrode is the same AC signal driving the piezoelectric crystals. This signal is changed into a series of standard  $-0.85$  V NIM pulses of the same frequency by a discriminator. The pre-scaler suppresses all but one of every  $N$  of these pulses, where  $N$  is selectable from 1 to 15; the pulse not suppressed appears at the output as a square NIM pulse of one cycle width. Several pre-scalings in series allow the number of suppressed cycles to be increased. The pulse generator can change the width and phase with respect to the driving oscillation of this pulse. The charging electrode driver changes the amplitude and bias of the pulse; it can apply an arbitrary potential to the charging electrode with a measured accuracy of  $10\mu V$ . The output of the discriminator is also fed to a logical AND circuit and a gate in series. The output of the gate, which is the second input of the AND, is normally in the high logical state. The input of a pulse changes the output of the gate from the high state to the low state for a specifiable time and thereby forces the output of the AND into the low state for the same period. After this time period the gate returns to the high state, whereupon the first pulse passing from the AND sends the output of the gate back into the low state. The frequency of the series of pulses from the discriminator can be lowered in this manner. The lowered frequency of pulses coming from the AND is used to drive the strobe with which the droplets are observed.

The reservoir of the droplet generator is pressurized to approximately 30 psi with Argon gas. The regulation of the pressure is important because the velocity of the stream is dependent on the pressure. The pressure is regulated by a constant-bleed regulator in series with a standard regulator and is steady to about 0.1%. The variation in pressure due to the changing height of the column of mercury in the reservoir is gradual and steady and less than 10%/hour. The time-scale of analysis is limited by the loss of resolution due to the change in velocity associated with this variation in pressure. Pressure valves on the electrode housing and the mercury trap guard against catastrophic increases in pressure in the apparatus. Both valves trip at a pressure 3 psi over atmospheric.

The deflecting electrodes are 36-inch sections of inch-wide, sixteenth-inch-thick chrome-plated ground steel. The geometry of the electrodes is detailed in Figure 7. The electric field used in actual operation is produced by a 3 kV potential across the electrodes. The resulting difference between the deflections of adjacent integer charges is predicted to be 0.7 mm. All

areas of low radius of curvature must be removed from the electrodes before operation in order to minimize field-ion emission associated with the intensified electric field at these points. The corners and edges of the steel were rounded prior to plating, and the chrome itself is smooth to 60-*L* specification ( $\approx 80 \text{ \AA}$  peak-to-peak variation). The ion-bombardment associated with the field-emission erodes any points on the negative deflecting electrode to an extent dependent on the magnitude of the applied electric field. In this manner, the deflecting electrodes are electro-polished before use by a 10 *kV* potential of each polarity, applied across the electrodes until the ion-current between them disappears.

The molecular sieve, Zeolite, used in the evacuation of the apparatus will absorb most vapors when cooled to *LN*<sub>2</sub> temperatures. The system is mechanically pumped down to a pressure of 100  $\mu$  *Hg* before exposing the Zeolite. This reduces the concentration of the few elements Zeolite is unable to absorb and so allows realization of the required 2  $\mu$  *Hg* pressure. The vapor from the housing passes through the mercury trap, which is filled with copper wool. The copper amalgamates with any mercury vapor present and so removes the vapor from the system. The remaining vapor passes into a *LN*<sub>2</sub> cold trap, where it is exposed to the Zeolite. The Zeolite pump contributes no vibrational noise to the system.

The photo-ejection of charges from the droplets might lead to a build-up of static electric charge on the dielectric inside surface of the housing pipe. This charge would have unpredictable effects on the trajectories of the charged droplets. A thin, electrically grounded layer of conductive graphite coating the inside of the housing pipe prevents such a buildup of charge. The observation windows in the apparatus are screened off with stainless steel mesh to complete the electrostatic shielding and at the same time preserve the transparency of the windows. The resistance of the graphite layer is on the order of 100 *k*  $\Omega$ /*ft*. Precautions were taken to minimize the photo-ejection of charge by making the apparatus opaque to ultra-violet light. The observation windows are made of *UV*-absorbing acrylic, and any *UV*-leaks into the apparatus are blacked over. The analysis of the droplets takes place in a light-tight box fixed at the bottom of the housing pipe.

The initial analysis of droplet charge will be made with a simple still camera. The film is exposed to light reflected from the droplets for a period of the order of a minute. The light illuminating the droplets is from a strobe synchronized to the rate of passage of droplets. The intensity of the image of a stream of deflected droplets depends on the number of droplets in the stream. Brighter streams are most likely to be those of integrally-charged droplets; any fainter stream between integer streams might correspond to a fractional charge.

The data are taken with a 1728-bucket optically-sensitive charge-coupled device (*CCD*). Light from a gas laser is scattered from the droplets onto the array of buckets. Each bucket

develops a charge which is proportional to the amount of light incident during the period of data accumulation. This period corresponds to the passage of a few droplets through the beam. Each bucket is in two sections in order to be able to collect new data while old data is being analyzed. A "start-of-scan" signal from the *CCD* relocates the charges to the lower half of the array, and the data analysis is initiated. The charges in the array of buckets are all physically shifted, in steps of one bucket, to the end of the array, where the contents of each bucket can be individually amplified and fed into a discriminator. The *CCD* is set to initiate a new round of data analysis as soon as the contents of all the buckets from the previous scan have been read. The discriminator outputs a standard high *TTL* pulse upon reception of a signal of amplitude greater than  $\approx 0.1$  *V*. The pulse height delivered from the passage of one droplet is  $\approx 0.3$  *V*. The discriminator output is fed to a multichannel analyzer, which sorts incoming pulses into its 1024 storage bins according to time of arrival. The "start-of-scan" signal from the *CCD* defines the zero of time for the multichannel analyzer. The multichannel analyzer can accept and store only one pulse per definable period of time. The smallest period definable is 10  $\mu$ sec, corresponding to a maximum rate of pulse analysis of 100 kHz. However, the *CCD* outputs the data from the array at rates between 156 kHz and 10 MHz. Running the multichannel analyzer at its maximum rate and the *CCD* at its lowest rate produces acceptable results. The low rate of analysis of *CCD*-bucket contents allows noise of the order of 0.01 *V* to build up in the buckets.

## 5. Conclusion

No data had been taken up to the time of publication. From the tests made of the apparatus we feel that the predicted sensitivity of  $10^{-24}$ /nucleon can be attained. The apparatus is designed to produce a separation of  $\approx 700$   $\mu$ m between adjacent integer charges. Earlier calculations of the magnitude of random effects on the trajectories of the droplets show that the maximum variance of a charged droplet from its unperturbed trajectory is 8  $\mu$ m; thus, an accuracy of better than  $0.02e$  can be achieved with the apparatus as described above.<sup>1</sup>

## Acknowledgements

I would like to thank Greg Hirsch and Ray Hagstrom of LBL for their help in the preparation of this document.

Prepared for the U.S. Department of Energy under Contract W-7405-ENG-48

## References

1. G. Hirsch, R. Hagstrom, C. Hendricks, *LBL Report No. LBL-9350*, 1979 (unpublished).
2. L. W. Jones, "A Review of Quark Search Experiments", *Reviews of Modern Physics*, **49**, 717 (1977).
3. H. C. Lee, "Drop Formation in a Liquid Jet", *IBM Journal of Research and Development*, **18**, 364 (1974).
4. W.T. Pimbley and H.C. Lee, "Satellite Droplet Formation in a Liquid Jet", *IBM Journal of Research and Development*, **21**, 21 (1977).
5. R. Bland (personal communication).

### Figure Captions

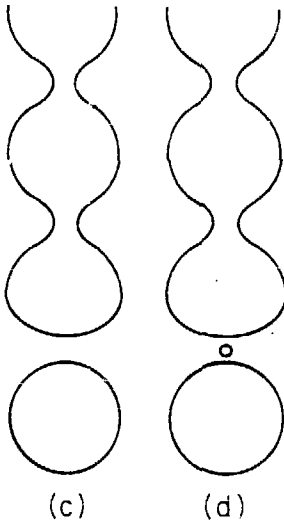
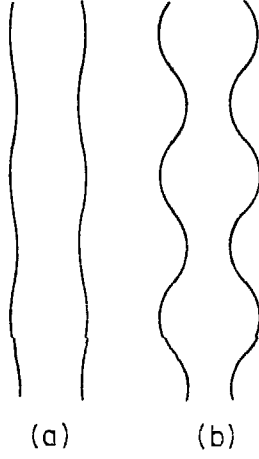
- Fig. 1. **Capillary-wave growth.** A capillary-wave perturbation applied to a cylindrical stream of liquid (*a*) will grow (*b*) until droplets are formed (*c*). The radius of the stream is given by  $r(z) = a + \rho(t) \sin(kz)$ , where  $a$  is the radius of the liquid stream,  $\rho(t)$  is the time-varying amplitude of the capillary-wave perturbation, and  $z$  is measured along the axis of the stream. Certain combinations of amplitude and frequency of capillary-wave perturbation induce the production and retention of satellite droplets between primary droplets (*d*). The satellites are formed from the isthmus of liquid between primary droplets.
- Fig. 2. **The dependence of the rate of growth  $\nu$  on the wave-number  $k$  of capillary-wave perturbations.** The value of  $\nu$  is real only between  $k=0$  and  $k=1/a$ , where  $a$  is the radius of the stream of liquid.
- Fig. 3. **Diagram of conditions governing satellite production.** The expression  $\lambda/d$  is the ratio of capillary-wave perturbation wavelength to the diameter of the liquid stream;  $t_b$  is the time to break-off of the droplets and is logarithmically related to capillary-wave amplitude. The infinity condition is the condition under which satellites do not merge with a primary droplet. Copyright 1977 by International Business Machine Corporation; reprinted with permission.
- Fig. 4. **Apparatus.** The droplet generator consists of the reservoir (*R*), the throat (*T*) and the orifice (*N*). The orifice is a small hole cut into a thin stainless steel sheet. The pre-fill tank (*F*) is a mercury storage tank that facilitates transfer of mercury to the reservoir without breaking the vacuum in the reservoir. The gas-pressure regulator (*C*) is a Conoflow *H 20XT* constant-bleed regulator in series with a standard regulator (*REG*). The *PZT* piezoelectric crystals ( $C_1, C_2$ ) are powered by the output of an oscillator (*Osc*, Tektronix *FG504*, 40 MHz function generator) which is amplified ( $A_1$ ) and sent through a 100:1 step-up transformer (*ST*). The charging electrode (*CE*) is a cylinder concentric to the stream of liquid, completely surrounding the orifice. The initial driving signal for the charging electrode is supplied by the oscillator (*Osc*). This signal is sent through a discriminator ( $D_1$ , model 157 dual end/or), into a pre-scaler (*P*) designed and constructed by Jerry Van Polen of Lawrence Berkeley Laboratory. It is then fed to a pulse generator (*PG*, model 18X1401P1), amplified ( $A_2$ ) and fed to the electrode. The amplifier is powered (*AP*) by a Power Designs model 2005 precision power source. The signal from the discriminator is also fed through an *AND* (*A*) and a gate (*G*) into the strobe (*L*). The *AND* and gate are contained in a Tektronix type 585 oscilloscope. The microscope (*MD*) consists of a Tiyoga 0.08, 3X objective and a Kompens 25X eyepiece. The deflecting sphere

(*DS*) is made of silver-plated brass. The collection wells (*SF*<sub>1</sub>,*SF*<sub>2</sub>) are constructed of stainless-steel sheet. The liquid collected in the wells is directed out of the apparatus into a storage tank (*PD*). The high voltage supply (*HV*) for the deflecting electrodes (*DE*) is a standard current-limited 8 *kV MWPC* power supply. A ten-foot section of 3-inch *ID PVC* pipe (*H*) houses the deflecting electrodes. Observation windows in the side of the pipe allow visual inspection of the droplets. The deflected droplets are analyzed through the camera viewing port (*V*). The charge-coupled device (*CCD*) is a Fairchild LineScan camera, model *CCD 1410*, donated courtesy of Howard Murphy of Fairchild Semiconductor. It is equipped with a Canon *TV-16 50 mm f/1.4* lens. The laser is a Spectra-Physics model *143-01 4mW* He-Ne laser. The multichannel analyzer (*MA*) is a Davidson model *1056A* multichannel analyzer. The mercury disposal system (*S*) collects and disposes of the mercury without breaking the vacuum in the housing. The pumping system consists of the mechanical pump (*MP*), the mercury trap (*M*) and the cold trap in a *LN*<sub>2</sub> bath (*CT*), one lobe of which is filled with Zeolite (*Z*). Two pressure valves (*PV*) relieve high pressures in the apparatus.

Fig. 5. **Mode of vibration of the piezoelectric crystals.**

Fig. 6. **Exploded view of droplet-generator throat.**

Fig. 7. **Geometry of deflecting electrodes.**



XBl 802-325

Figure 1

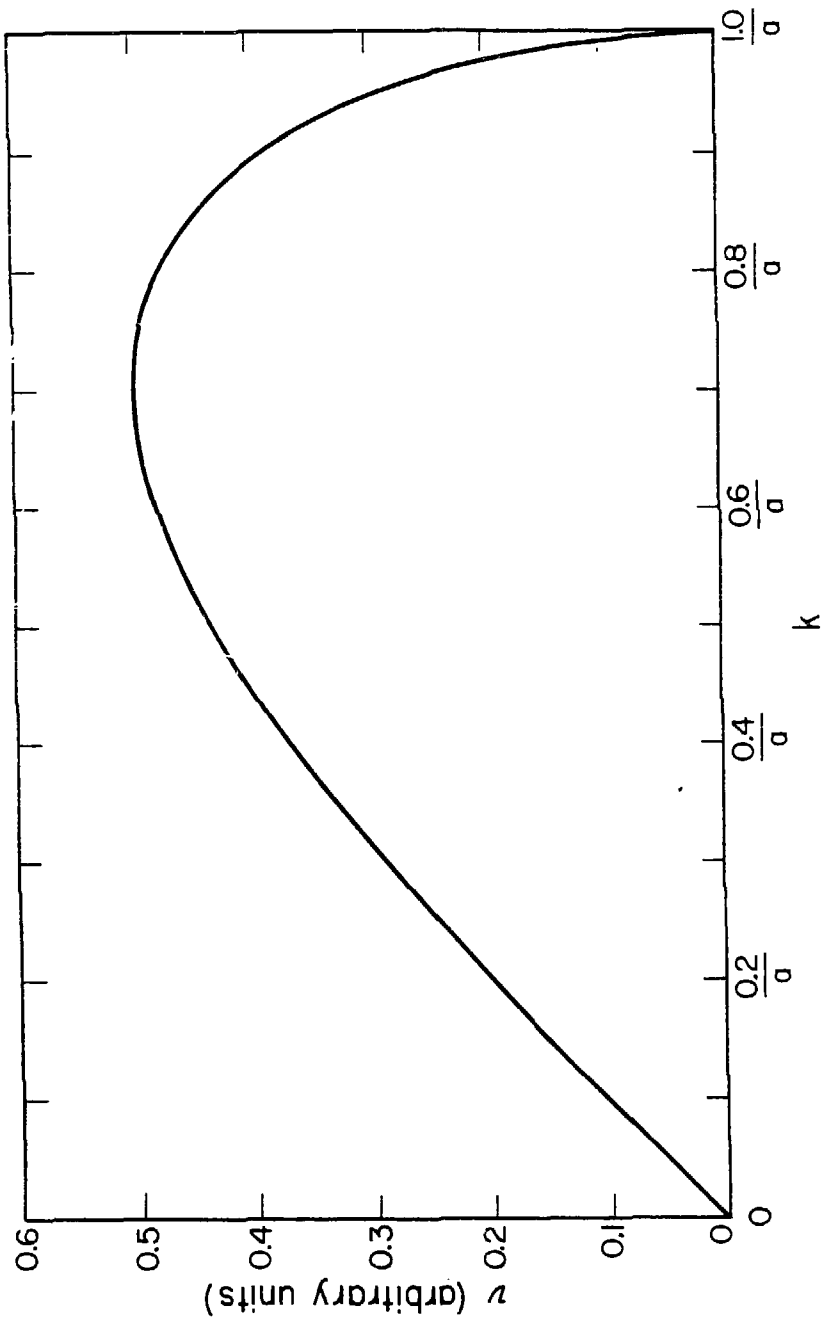


Figure 2

XBL 802 324

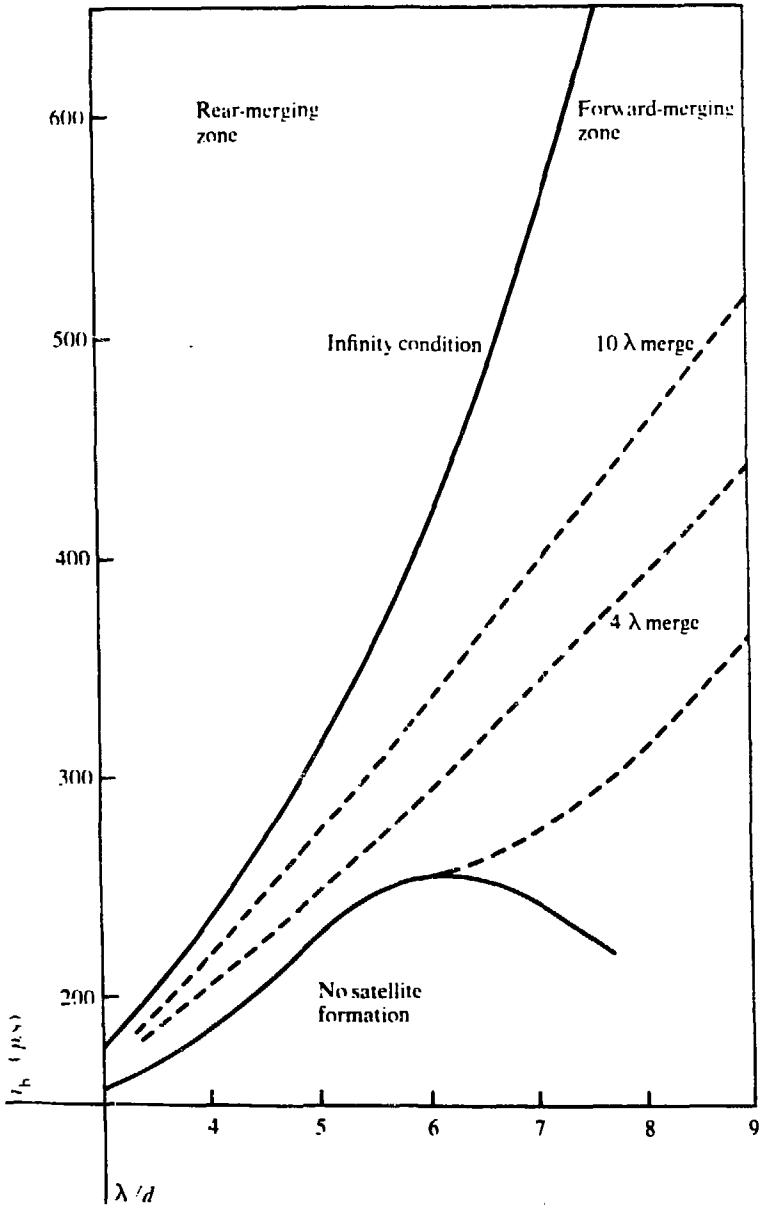
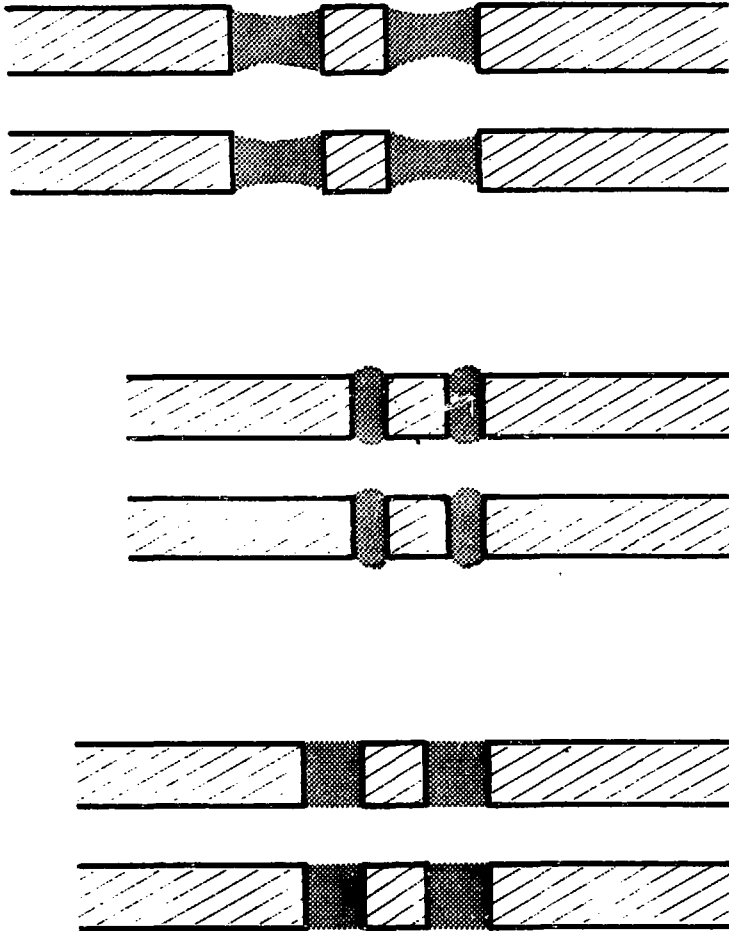


Figure 3

XBL 803-8625





XBL 802-326

Figure 5

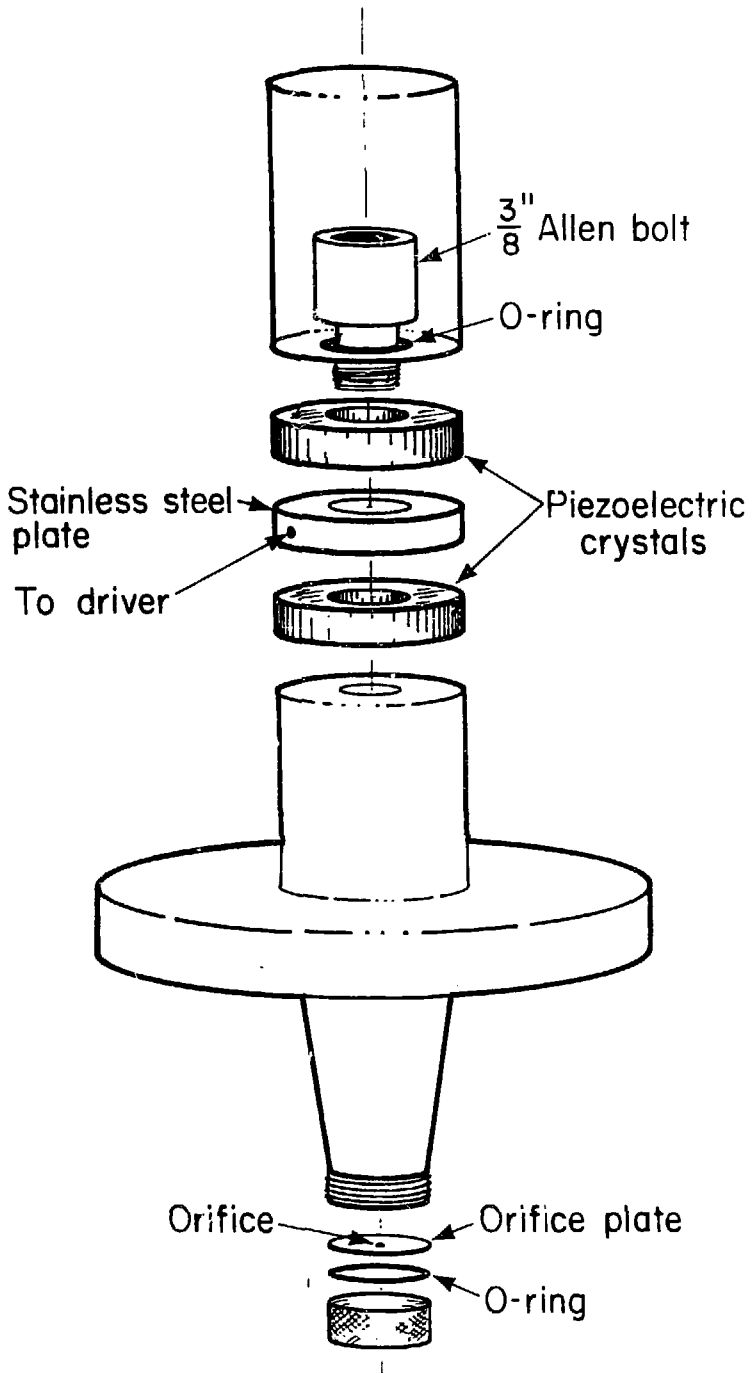
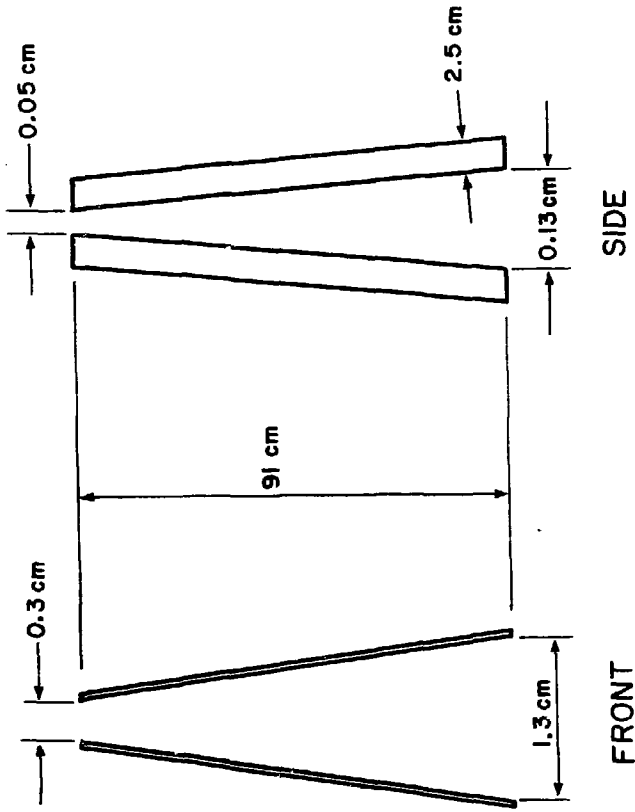


Figure 6

XBL 802-328



*Not to scale*

XBL 802-327

Figure 7